

Measurement of $\Gamma(K_{\mu 3})/\Gamma(K_{e 3})$ ratio using stopped positive kaons

K. Horie ^{a,*}, S. Shimizu ^a, M. Abe ^b, M. Aoki ^c, I. Arai ^d,
 Y. Asano ^b, T. Baker ^c, M. Blecher ^e, M.D. Chapman ^c,
 P. Depommier ^f, M. Hasinoff ^h, H.C. Huang ⁱ, Y. Igarashi ^{d,c,1},
 T. Ikeda ^{d,j,1}, J. Imazato ^c, A.P. Ivashkin ^g, M.M. Khabibullin ^g,
 A.N. Khotjantsev ^g, Y.G. Kudenko ^g, Y. Kuno ^{c,a,1}, J.-M. Lee ^k,
 K.S. Lee ^l, A.S. Levchenko ^g, G.Y. Lim ^c, J.A. Macdonald ^m,
 C.R. Mindas ⁿ, O.V. Mineev ^g, Y.-H. Shin ^k, Y.-M. Shin ^m,
 A. Suzuki ^d, A. Watanabe ^d, and T. Yokoi ^{o,c,1}

KEK-E246 Collaboration

^a *Department of Physics, Osaka University, Osaka 560-0043, Japan*

^b *Institute of Applied Physics, University of Tsukuba, Ibaraki 305-0006, Japan*

^c *IPNS, High Energy Accelerator Research Organization (KEK), Ibaraki 305-0801, Japan*

^d *Institute of Physics, University of Tsukuba, Ibaraki 305-0006, Japan*

^e *Department of Physics, Virginia Polytechnic Institute and State University, VA 24061-0435, U.S.A.*

^f *Laboratoire de Physique Nucléaire, Université de Montréal, Montréal, Québec, Canada H3C 3J7*

^g *Institute for Nuclear Research, Russian Academy of Sciences, Moscow 117312, Russia*

^h *Department of Physics and Astronomy, University of British Columbia, Vancouver, Canada V6T 1Z1*

ⁱ *Department of Physics, National Taiwan University, Taipei 106, Taiwan*

^j *The Institute of Physical and Chemical Research, Saitama 351-0106, Japan.*

^k *Department of Physics, Yonsei University, Seoul 120-749, Korea*

^l *Department of Physics, Korea University, Seoul 136-701, Korea*

^m *TRIUMF, Vancouver, British Columbia, Canada V6T 2A3*

ⁿ *Department of Physics, Princeton University, NJ 08544, U.S.A.*

^o *Department of Physics, University of Tokyo, Tokyo 113-0033, Japan*

Abstract

The ratio of the $K^+ \rightarrow \pi^0 \mu^+ \nu$ ($K_{\mu 3}^+$) and $K^+ \rightarrow \pi^0 e^+ \nu$ ($K_{e 3}^+$) decay widths, $\Gamma(K_{\mu 3})/\Gamma(K_{e 3})$, has been measured with stopped positive kaons. $K_{\mu 3}^+$ and $K_{e 3}^+$ samples containing 2.4×10^4 and 4.0×10^4 events, respectively, were analyzed. The $\Gamma(K_{\mu 3})/\Gamma(K_{e 3})$ ratio was obtained to be $0.671 \pm 0.007(\text{stat.}) \pm 0.008(\text{syst.})$ calculating the detector acceptance by a Monte Carlo simulation. The coefficient of the q^2 dependent term of the f_0 form factor was also determined to be $\lambda_0 = 0.019 \pm 0.005(\text{stat.}) \pm 0.004(\text{syst.})$ with the assumption of μ - e universality in $K_{l 3}^+$ decay. The agreement of our result with the λ_0 value obtained from $K_{\mu 3}^+$ Dalitz plot analyses supports the validity of the μ - e universality.

1 Introduction

The spectroscopic studies to determine form factors of the K^+ semi-leptonic decays, $K^+ \rightarrow \pi^0 l^+ \nu$ ($K_{l 3}^+$), are of importance both in studying low energy properties of the strong interaction in terms of effective theories [1,2], and also in studying fundamental interactions. In our previous work [3], we reported a result testing the exotic couplings in $K^+ \rightarrow \pi^0 e^+ \nu$ ($K_{e 3}^+$) decay, showing the non existence of scalar and tensor interactions, contradicting the current world average adopted by Particle Data Group [4]. In the present work, the $K^+ \rightarrow \pi^0 \mu^+ \nu$ ($K_{\mu 3}^+$) events, which were collected simultaneously, were analyzed to determine the ratio of the $K_{\mu 3}^+$ and $K_{e 3}^+$ decay widths $\Gamma(K_{\mu 3})/\Gamma(K_{e 3})$. This quantity is one of the most important observables to evaluate the $K_{l 3}^+$ form factors.

Assuming that only the V–A interaction contributes to the $K_{l 3}$ decay, the decay amplitude can be described by two dimensionless form factors, $f_+(q^2)$ and $f_0(q^2)$, which are functions of the momentum transferred to the leptons $q^2 = (P_K - P_{\pi^0})^2$ where P_K and P_{π^0} are the four momenta of the K^+ and π^0 , respectively. They are given as,

$$\begin{aligned} f_+(q^2) &= f_+(0)[1 + \lambda_+(q/m_\pi)^2], \\ f_0(q^2) &= f_0(0)[1 + \lambda_0(q/m_\pi)^2]. \end{aligned}$$

Assuming μ - e universality, the form factors between $K_{\mu 3}$ and $K_{e 3}$ decays are identical and $\Gamma(K_{\mu 3})/\Gamma(K_{e 3})$ can be written as [5],

* Corresponding author.

E-mail address: kate@phys.wani.osaka-u.ac.jp (Keito HORIE)

¹ Second institutions are present addresses.

$$\begin{aligned} \Gamma(K_{\mu 3})/\Gamma(K_{e 3}) = & 0.6457 - 0.1531\lambda_+ \\ & + 1.5646\lambda_0 + O(\lambda_+^2 + \lambda_+\lambda_0 + \lambda_0^2). \end{aligned} \quad (1)$$

This equation cannot determine the λ_+ and λ_0 parameters uniquely but simply fixes a relationship between them. However, if the λ_+ value derived from K_{e3} data analyses is assumed, the λ_0 parameter can be obtained from Eq. (1). In this analysis, our K_{e3} result for the λ_+ parameter, $\lambda_+ = 0.0278 \pm 0.0040$, was employed [3].

It should be noted that the λ_0 parameter can be also determined by studying the Dalitz plot distribution of $K_{\mu 3}$ decay or the muon polarization in $K_{\mu 3}$ decay [4]. The determination of the λ_0 parameter from the $\Gamma(K_{\mu 3})/\Gamma(K_{e 3})$ ratio is based on the assumption of μ - e universality. This is not the case for the other two methods. Thus, μ - e universality in K_{l3} decay can be tested by comparing the λ_0 parameter obtained from a branching ratio measurement λ_0^{br} with that obtained from a Dalitz plot measurement λ_0^{dal} and/or μ^+ polarization measurement λ_0^{pol} . In this case, however, a precise acceptance function has to be carefully determined over the whole Dalitz space for the $K_{\mu 3}$ Dalitz plot analysis.

In this letter, we present a new precise measurement of the $\Gamma(K_{\mu 3})/\Gamma(K_{e 3})$ branching ratio and the λ_0 parameter. The experiment used a stopped K^+ beam in conjunction with a 12-sector iron-core superconducting toroidal spectrometer [6]. $\Gamma(K_{\mu 3})/\Gamma(K_{e 3})$ was obtained by measuring the ratio of the number of accepted $K_{\mu 3}$ and $K_{e 3}$ events corrected for detector acceptance.

2 Experiment

The experiment was performed at the KEK 12 GeV proton synchrotron. The experimental apparatus was constructed for a T-violation search in $K_{\mu 3}$ decay [7]. A schematic cross sectional side view of the detector is shown in Fig. 1. We detected both of the π^0 decay gammas which enabled us to reconstruct the complete kinematics of a K_{l3} event in contrast to the previous experiment [8]; this increased the reliability of the event selection. Because of the rotational symmetry of the 12 identical gaps in the spectrometer and the large directional acceptance of the π^0 detector [9], distortions due to detector acceptance were drastically reduced. Moreover, the similarity of the $K_{\mu 3}$ and $K_{e 3}$ kinematics reduced the systematic error due to the imperfect reproducibility of the experimental conditions in the simulation of the ratio of the calculated acceptance for the $K_{\mu 3}$ and $K_{e 3}$ decays. The measurement was carried out for two values of the central magnetic field strength, $B=0.65$ and 0.90 T, yielding a consistency check with regard to the spectrometer acceptance and energy loss estimation in the target.

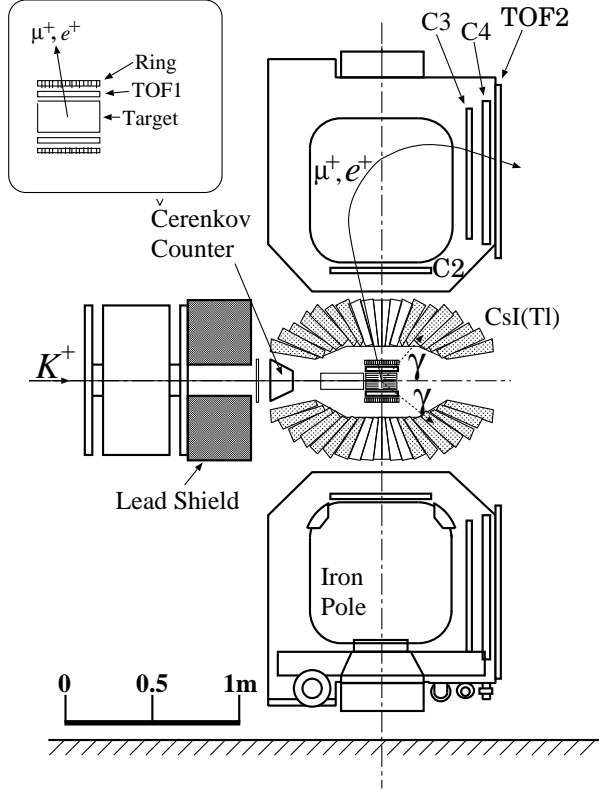


Fig. 1. Cross sectional side view of the E246 setup. Assembly detail of the active target, TOF1, and ring counter is shown in the inset.

$K_{\mu 3}$ ($K_{e 3}$) events were identified by analyzing the μ^+ (e^+) momentum with the spectrometer and detecting the two photons in the CsI(Tl) calorimeter. Charged particles from the target were tracked and momentum-analyzed using multi-wire proportional chambers (MWPCs) at the entrance (C2) and exit (C3 and C4) of the magnet gap, as well as by the active target and an array of ring counters [10] surrounding the target. Particle identification between the μ^+ s and e^+ s was carried out by time-of-flight (TOF) between TOF1 and TOF2 scintillation counters. TOF1 surrounds the active target and TOF2 is located at the exit of the spectrometer. The π^0 detector, an assembly of 768 CsI(Tl) crystals, covers 75% of the total solid angle. Since photons produce electromagnetic showers, their energy was shared among several crystals. The photon energy and hit position were obtained by summing the energy deposits and energy-weighted centroid, respectively. Timing information from each module was used to identify a photon cluster and to suppress accidental backgrounds due to beam particles. The two-photon invariant mass ($M_{\gamma\gamma}$) and the π^0 energy and direction were obtained from the photon momentum vectors.

$K_{\mu 3}$ and $K_{e 3}$ decays at rest were selected by the following procedure, which is similar to our $K_{e 3}$ study. The K^+ decay time, defined as the charged lepton signal at the TOF1 counter, was required to be more than 5 ns later than the

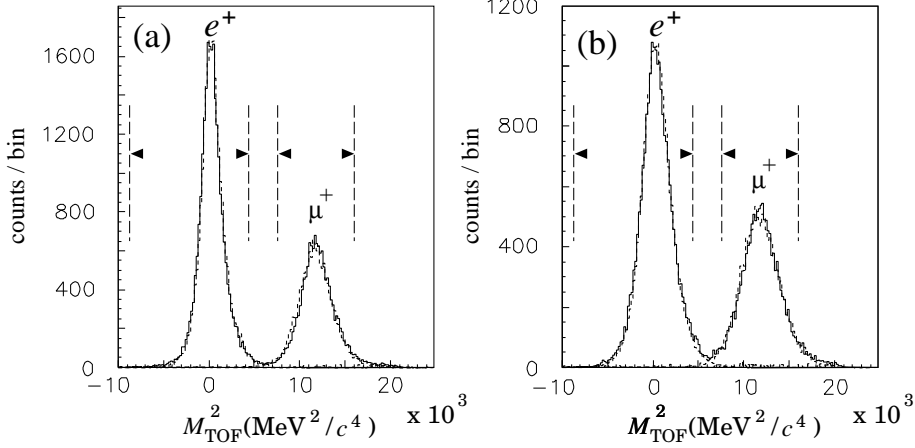


Fig. 2. Mass squared spectra M_{TOF}^2 obtained in TOF analysis for all momenta at (a)0.65 and (b)0.90 T. The solid line is the experimental data and the dotted line is the Monte Carlo simulation. The Monte Carlo data are scaled by the obtained $\Gamma(K_{\mu 3})/\Gamma(K_{e 3})$ value. The μ^+ and e^+ selection regions are indicated by the dashed lines.

K^+ arrival time measured by the Čerenkov counter to remove in-flight K^+ decays. Events with π^+ decays in-flight and scattering of charged particles from the magnet pole faces were eliminated by a track consistency cut in the ring counters. Events with two clusters in the CsI(Tl) calorimeter were selected as π^0 decays and events with other cluster numbers were rejected. The acceptance cut on the invariant mass was $50 < M_{\gamma\gamma} < 140 \text{ MeV}/c^2$. Requirements for the charged particle momentum corrected for the energy loss in the target ($P_{\text{cor}} < 175 \text{ MeV}/c$) plus opening angle between a charged particle and the π^0 ($\theta_{l+\pi^0} < 154^\circ$) removed the $K_{\pi 2}$ events.

The mass squared (M_{TOF}^2) of the charged particles, obtained from the TOF and momentum, are shown in Fig. 2 integrated over the entire momentum region. The μ^+ and e^+ selection regions are also indicated in the figure. The timing resolution of $\sigma_T = 270 \text{ ps}$ provides a good separation between the $K_{\mu 3}$ and $K_{e 3}$ events. It should be emphasized that only these requirements were imposed for the $K_{\mu 3}$ and $K_{e 3}$ event extraction. The numbers of good events after those cuts mentioned above are 12882(10704) and 23122(16850) at 0.65(0.90) T for $K_{\mu 3}$ and $K_{e 3}$ decays, respectively, where small fractions due to the background events are still included. Fig. 3 and 4 show the $K_{\mu 3}$ and $K_{e 3}$ spectra for the setting of B=0.65 and 0.90 T, respectively.

3 Monte Carlo simulation

In order to obtain the detector acceptance and estimate the background fraction, the Monte Carlo simulation was carried out for both the charged particle

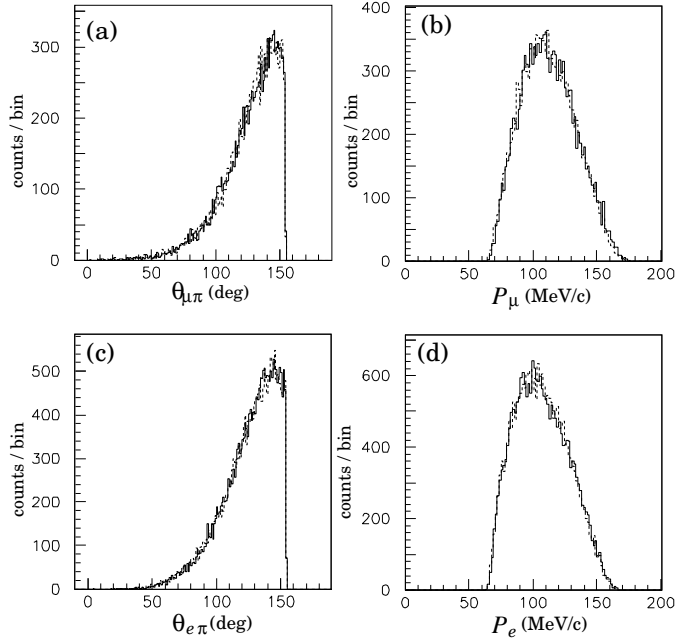


Fig. 3. Spectra of the selected events (solid line): (a) $\theta_{\mu+\pi^0}$, (b) P_{μ^+} for $K_{\mu 3}$ decay and (c) $\theta_{e+\pi^0}$, (d) P_{e^+} for $K_{e 3}$ decay, and Monte Carlo simulation (dotted line). They were obtained for the setting of $B=0.65$ T.

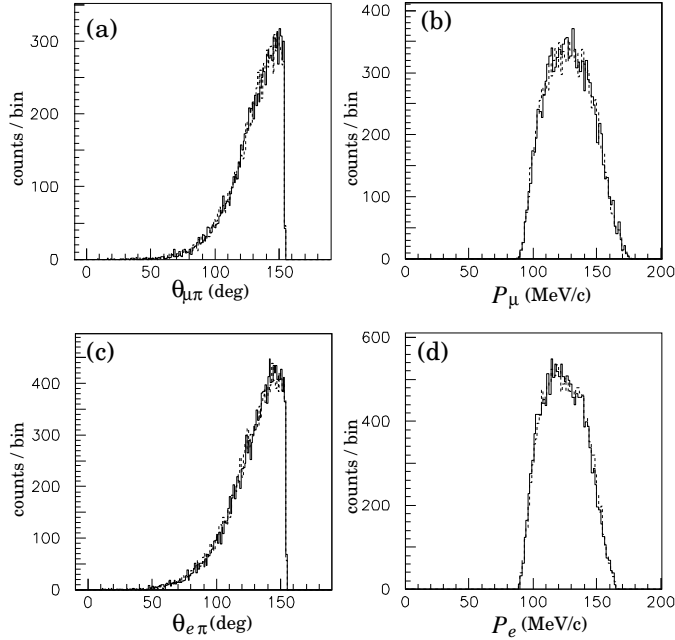


Fig. 4. Spectra of the selected events (solid line): (a) $\theta_{\mu+\pi^0}$, (b) P_{μ^+} for $K_{\mu 3}$ decay and (c) $\theta_{e+\pi^0}$, (d) P_{e^+} for $K_{e 3}$ decay, and Monte Carlo simulation (dotted line). They were obtained for the setting of $B=0.90$ T.

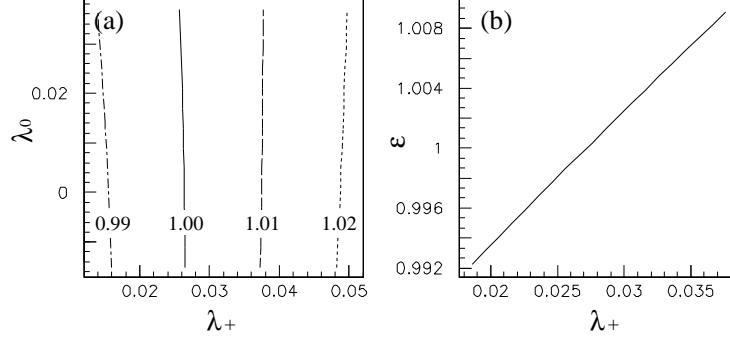


Fig. 5. The correction factor for the detector acceptance for the setting of $B=0.65$ T; (a) ϵ contour in terms of the λ_+ and λ_0 parameters for $K_{\mu 3}$ and (b) dependence on the λ_+ parameter for $K_{e 3}$. The correction factor for the setting of $B=0.90$ T is similar.

measurement by the spectrometer and the π^0 measurement by the CsI(Tl) detector. The initial Dalitz distributions were generated with the values of $\lambda_+ = 0.0278$ and the current world average $\lambda_0 = 0.006$, while the Dalitz distribution of $K_{e 3}$ decay is insensitive to the λ_0 parameter. The radiative corrections were taken into account by following the Ginsberg procedure [11]. The simulation data were analyzed in the same manner as the experimental sample. The dotted lines in Fig. 3 and Fig. 4 show the simulation spectra for the setting of $B=0.65$ and 0.90 T, respectively, using the assumed λ_+ and λ_0 parameters. These spectra are normalized so that the total number of events is the same as the experimental one. Here, it is to be noted that much higher statistical accuracy for the Monte Carlo simulation is necessary to determine the form factors from the $K_{\mu 3}$ Dalitz plot analysis.

By using the simulation data, the detector acceptance (Ω) is calculated as,

$$\Omega = N_{\text{acc}}/N_{\text{gen}} \times \epsilon(\lambda_+, \lambda_0) \equiv \Omega^0 \times \epsilon(\lambda_+, \lambda_0),$$

where N_{acc} and N_{gen} are the number of events accepted by our event selection requirements and the number of generated K^+ events, respectively. Ω^0 denotes the detector acceptance at the assumed form factor for the production of the simulation samples. They were $\Omega^0(K_{\mu 3}) = (1.790 \pm 0.014) \times 10^{-3}$, $\Omega^0(K_{e 3}) = (2.161 \pm 0.014) \times 10^{-3}$ for the setting of $B=0.65$ T and $\Omega^0(K_{\mu 3}) = (1.669 \pm 0.014) \times 10^{-3}$, $\Omega^0(K_{e 3}) = (1.756 \pm 0.013) \times 10^{-3}$ for the setting of $B=0.90$ T. The detector acceptance depends only slightly on the form factor (*i.e.*, the shape of the Dalitz distribution), therefore a correction factor $\epsilon(\lambda_+, \lambda_0)$ is introduced. ϵ was calculated by taking into account the event selection requirements such as P_{cor} , $\theta_{l+\pi^0}$, and M_{TOF}^2 cuts. As shown in Fig. 5(a,b), the ϵ distribution for $K_{\mu 3}$ decay was obtained as a contour plot in the (λ_+, λ_0) space, while ϵ for $K_{e 3}$ decay was obtained as a function of the λ_+ parameter.

M_{TOF}^2 spectra were calculated by assuming a TOF resolution of $\sigma_T=270$ ps.

Table 1

Background fractions included in the $K_{\mu 3}$ and $K_{e 3}$ samples.

	background item	background fraction	
		B=0.65 T	B=0.90 T
$K_{\mu 3}$	$K_{\pi 2}$	0.6%	0.9%
	$K_{e 3}$	0.1%	0.1%
	$K_{\mu 3\gamma}$	< 0.1%	< 0.1%
	accidental	0.3%	0.3%
$K_{e 3}$	$K_{\pi 2}$	0.4%	0.3%
	$K_{\mu 3}$	< 0.1%	< 0.1%
	$K_{e 3\gamma}$	< 0.1%	< 0.1%
	accidental	0.3%	0.3%

They are shown as dotted lines in Fig. 2. Since the charged particles were identified by M_{TOF}^2 measurement, the choice of the TOF response function was important for the determination of the background contamination. We took into account $K_{\pi 2}$, $K_{e 3}$, $K_{\mu 3\gamma}$ decays for the $K_{\mu 3}$ background and $K_{\pi 2}$, $K_{\mu 3}$, $K_{e 3\gamma}$ decays for the $K_{e 3}$ background. The background fraction depends on the magnetic setting of the spectrometer, as summarized in Table 1. The most dominant background is due to $K_{\pi 2}$ decay in-flight. The accidental background fraction due to beam particles was estimated to be 0.3% for both $K_{\mu 3}$ and $K_{e 3}$ samples.

4 Results

The $\Gamma(K_{\mu 3})/\Gamma(K_{e 3})$ ratio can be written as,

$$\Gamma(K_{\mu 3})/\Gamma(K_{e 3}) = N(K_{\mu 3})/N(K_{e 3}) \cdot \Omega(K_{e 3})/\Omega(K_{\mu 3}),$$

where N is the number of accepted events after subtracting backgrounds. The λ_0 parameter can be determined by substituting the obtained $\Gamma(K_{\mu 3})/\Gamma(K_{e 3})$ value and $\lambda_+ = 0.0278$ into Eq. (1). However, the situation was a little more complicated because the $K_{\mu 3}$ acceptance also depends on the λ_0 parameter. Therefore, it was derived by iteration to minimize the difference between the λ_0 parameter for the acceptance determination (λ_0^{acc}) and the λ_0 parameter obtained from Eq. (1) (λ_0^{obt}). Fig. 6 shows the $|\lambda_0^{\text{acc}} - \lambda_0^{\text{obt}}|$ plot as a function of λ_0^{acc} for both the 0.65 and 0.90 T data. The value of λ_0^{acc} , which satisfied the condition of $|\lambda_0^{\text{acc}} - \lambda_0^{\text{obt}}| = 0$, was adopted as our final result. The λ_0 parameter and associated $\Gamma(K_{\mu 3})/\Gamma(K_{e 3})$ value are shown in Table 2 together with those

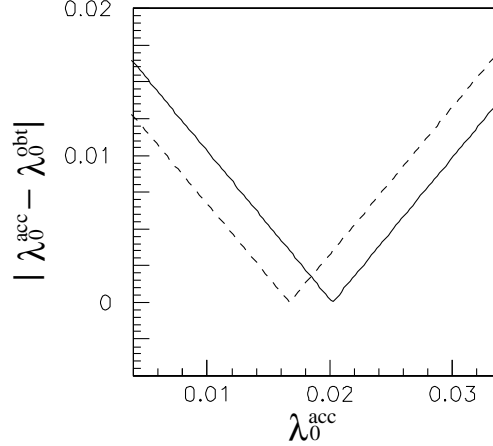


Fig. 6. $|\lambda_0^{\text{acc}} - \lambda_0^{\text{obt}}|$ plot as a function of λ_0^{acc} . The solid and dashed lines correspond to 0.65 and 0.90 T data, respectively. The value of λ_0^{acc} , which satisfied the condition of $|\lambda_0^{\text{acc}} - \lambda_0^{\text{obt}}| = 0$, was adopted as the final result.

Table 2

Results of $\Gamma(K_{\mu 3})/\Gamma(K_{e 3})$ and λ_0 parameter

	$\Gamma(K_{\mu 3})/\Gamma(K_{e 3})$	λ_0
0.65T	0.673 ± 0.010	0.020 ± 0.006
0.90T	0.668 ± 0.011	0.017 ± 0.007
combined	0.671 ± 0.007	0.019 ± 0.005
no μ - e universality assumption	0.669 ± 0.007	—
world average [4]	0.680 ± 0.013	0.006 ± 0.007

of the world average quoted in PDG. The results of B =0.65 and 0.90 T data were then combined by calculating the error weighted average as, $\lambda_0 = 0.019 \pm 0.005$ and $\Gamma(K_{\mu 3})/\Gamma(K_{e 3}) = 0.671 \pm 0.007$.

The systematic errors, which have been categorized into background contamination and inaccurate detector acceptance, are summarized in Table 3. The ambiguity of the $K_{\pi 2}$ fraction introduces a significant systematic error, while the other channels are negligible. If the $K_{\pi 2}$ background in the $K_{\mu 3}$ sample is not correctly evaluated, the results could strongly depend on the cut points of $\theta_{l\pi^0}$ and P_{cor} . The dependence on both cut points was treated as a systematic error. Also, an imperfect TOF response function in the simulation could introduce a systematic error, which would be concentrated around the tail part of the M_{TOF}^2 peaks. This contribution was also studied by the cut point dependence of the TOF window positions. The accidental backgrounds could be neglected because their fractions were small and common to both the $K_{\mu 3}$ and the $K_{e 3}$ events.

The systematic errors associated with the measurement, namely instrumental

Table 3
Systematic errors

	$\Delta[\Gamma(K_{\mu 3})/\Gamma(K_{e 3})]$	$\Delta\lambda_0$
[Background contamination]		
decay-in-flight from $K_{\pi 2}$ decay	0.004	0.003
TOF response	0.004	0.003
[Detector acceptance]		
instrumental misalignment	<0.001	<0.001
energy loss estimation in the target	<0.001	<0.001
experimental error of the $K_{e 3}$ λ_+ parameter	0.001	0.001
choice of the $K_{\mu 3}$ λ_+ parameter	0.005	–
total	0.008	0.004

systematic errors, are negligible. The effects due to misalignment of the CsI(Tl) barrel, K^+ target, and MWPCs and the contribution of misunderstanding of the energy loss of the charged particles in the target were estimated and found to be negligible. Differences in the detection efficiency for e^+ and μ^+ in the MWPCs would introduce a systematic error, which was studied by the sector number dependence of the spectrometer. The results obtained in the various sectors were distributed within statistical error, and this contribution was also estimated to be negligible. Since the detector acceptance depends on the λ_+ parameter, as well as the λ_0 parameter, the ambiguity of the λ_+ parameter introduced a systematic error. This effect was estimated using the ϵ distributions shown in Fig. 5. Using $\lambda_+ = 0.0278 \pm 0.0040$, the change of the $\epsilon(K_{\mu 3})/\epsilon(K_{e 3})$ value in this region was considered to be the systematic error. If the current world average $\lambda_+ = 0.031 \pm 0.008$ for $K_{\mu 3}$ decay [4] is used instead of taking the μ - e universality value of 0.0278, $\Gamma(K_{\mu 3})/\Gamma(K_{e 3})$ is shifted to 0.669 ± 0.007 through the modification of the $K_{\mu 3}$ acceptance. Although this shift (-0.002) is much smaller than the statistical error (0.007), the acceptance deformation due to the ambiguity of the $K_{\mu 3}$ λ_+ was included as an additional systematic error. These errors, regarding them as one standard deviation errors, are summarized in Table 3. The total size of the systematic errors was obtained by adding each item in quadrature. The total systematic errors for $\Delta[\Gamma(K_{\mu 3})/\Gamma(K_{e 3})]$ and $\Delta\lambda_0$ are 0.008 and 0.004, respectively, which are basically equal to the statistical error.

5 Conclusion

The ratio of the $K^+ \rightarrow \pi^0 \mu^+ \nu$ ($K_{\mu 3}^+$) and $K^+ \rightarrow \pi^0 e^+ \nu$ ($K_{e 3}^+$) decay widths, $\Gamma(K_{\mu 3})/\Gamma(K_{e 3})$, has been measured for stopped positive kaons. Assuming μ - e universality in $K_{l 3}^+$ decay, the coefficient of the q^2 dependent term of the f_0 form factor was determined from the measured $\Gamma(K_{\mu 3})/\Gamma(K_{e 3})$ ratio. In contrast to the previous experiments, a large detector acceptance and its symmetrical structure enabled us to reduce the statistical errors while suppressing the systematic errors. Our results are

$$\begin{aligned}\Gamma(K_{\mu 3})/\Gamma(K_{e 3}) &= 0.671 \pm 0.007(\text{stat.}) \pm 0.008(\text{syst.}), \\ \lambda_0 &= 0.019 \pm 0.005(\text{stat.}) \pm 0.004(\text{syst.}).\end{aligned}$$

The λ_0 parameter obtained from the present work is consistent with that from recent $K_{\mu 3}^+$ Dalitz plot analyses [13,14], which supports the validity of μ - e universality in $K_{l 3}^+$ decay. If the assumption of μ - e universality is removed, $\Gamma(K_{\mu 3})/\Gamma(K_{e 3})$ can be written as [5],

$$\begin{aligned}\Gamma(K_{\mu 3})/\Gamma(K_{e 3}) &= [g_{\mu} f_{+}^{\mu}(0)/g_e f_{+}^e(0)]^2 \\ &\times (0.6457 + 2.2342\lambda_{+}^{\mu} - 2.3873\lambda_{+}^e + 1.5646\lambda_0),\end{aligned}\quad (2)$$

where g is weak coupling constant for the lepton current. Substituting $\Gamma(K_{\mu 3})/\Gamma(K_{e 3}) = 0.669 \pm 0.011$ (present result with no μ - e universality assumption), $\lambda_{+}^{\mu} = 0.031 \pm 0.008$ (the current world average), $\lambda_{+}^e = 0.0278 \pm 0.0040$ (our $K_{e 3}$ result), and $\lambda_0 = 0.039 \pm 0.011$ (error weighted average of Ref. [13] and [14]) into Eq. (2), $g_{\mu} f_{+}^{\mu}(0)/g_e f_{+}^e(0)$ is derived to be 0.971 ± 0.019 which is consistent with unity within the experimental error. From the viewpoint of the theoretical framework, the $K_{l 3}^+$ form factors are of importance in studying low energy properties of the strong interaction in terms of effective theories. The predicted values of the λ_0 parameter are $\lambda_0 = 0.017 \pm 0.004$ [1] and $\lambda_0 = -0.03$ [2]. The present result is consistent with the former and inconsistent with the latter. Also, the $\Delta I = 1/2$ rule leads to identical λ_0 parameters between $K_{l 3}^+$ and $K_{l 3}^0$ decays [12]. The λ_0 parameter from the $K_{l 3}^0$ analyses has been determined to be $\lambda_0 = 0.025 \pm 0.006$ [4], which is consistent with the present result.

Acknowledgements

This work has been supported in Japan by a Grant-in-Aid from the Ministry of Education, Science, Sports and Culture, and by JSPS; in Russia by the Ministry of Science and Technology, and by the Russian Foundation for Basic Research; in Canada by NSERC and IPP, and by the TRIUMF infrastructure support provided under its NRC contribution; in Korea by BSRI-MOE and KOSEF; in the U.S.A by NSF and DOE; and in Taiwan by NSC. The authors gratefully acknowledge the excellent support received from the KEK staff.

References

- [1] J. Gasser and H. Leutwyler, Nucl. Phys. **B250**, 517 (1985).
- [2] D.I. Kazakov, V.N. Pervushin, and M.K. Volkov, Phys. Lett. **B64**, 201 (1976).
- [3] S. Shimizu *et al.*, Phys. Lett. **B495**, 33 (2000).
- [4] Particle Data Group, Eur. Phys. J. **C15**, Review of Particle Physics (2000).
- [5] H.W. Fearing, E. Fischbach, and J. Smith, Phys. Rev. **D2**, 542 (1970); Phys. Rev. Lett. **24**, 189 (1970).
- [6] J. Imazato *et al.*, in *Proceedings of the 11th International Conference on Magnet Technology* (Elsevier Applied Science, London, 1990), p.366.
- [7] M. Abe *et al.*, Phys. Rev. Lett. **83**, 4253 (1999).
- [8] J. Heintze *et al.*, Phys. Lett. **B70**, 482 (1977).
- [9] D.V. Dementyev *et al.*, Nucl. Instr. Method **A440**, 151 (2000).
- [10] A.P. Ivashkin *et al.*, Nucl. Instr. Method **A394**, 321 (1997).
- [11] E.S. Ginsberg, Phys. Rev. **42**, 1035 (1966).
- [12] L.B. Auerbach *et al.*, Phys. Rev. **155**, 1505 (1967).
- [13] R. Whitman *et al.*, Phys. Rev. **D21**, 652 (1980).
- [14] V.M. Artemov *et al.*, Physics of Atomic and Nuclei. **60** 2023 (1997)